NEW NA48/2 RESULTS ON RARE KAON DECAYS*

Sergey Shkarovskiy

for NA48/2 Collaboration†

Joint Institute for Nuclear Research, Dubna, Russia
Sergey.Shkarovskiy@cern.ch

(Received August 19, 2019)

NA48/2 results related to ChPT testing are presented. The most precise measurement of the charged kaon semileptonic form factors has been obtained from 4.4×10^6 the $K^\pm \to \pi^0 e^\pm \nu_e$ ($K^\pm_{e3}$) and 2.91×10^6 the $K^\pm \to \pi^0 \mu^\pm \nu_\mu$ ($K^\pm_{\mu 3}$) events collected in 2004. In addition, the branching ratio of the $K^\pm \to \pi^\pm \pi^0 e^+ e^-$ decay, that has not been observed so far, has been obtained from a sample of 4919 decay candidates with 4.9% background. The branching ratio in the full kinematic region is measured to be $(4.24 \pm 0.15) \times 10^{-6}$, which is in agreement with ChPT predictions.

DOI:10.5506/APhysPolBSupp.13.89

1. Introduction

The NA48/2 experiment at the CERN SPS was designed to search for direct CP violation in $K^\pm$ decays to three pions [1, 2]. Two simultaneous beams of charged particles containing nearly 6% of $K^\pm$ were produced by 400 GeV/c protons impinging on a beryllium target. Particles of opposite charge with a central momentum of 60 GeV/c and a momentum band of $\pm 3.8\%$ (r.m.s.) were selected by a system of magnets and collimators. Two resulting beams, each ≈ 1 cm wide, were superimposed in the decay volume inside a 114 m long vacuum tank.

The main components of the NA48/2 detector were a magnetic spectrometer, composed of four drift chambers (DCH1–DCH4) and a dipole magnet. The spectrometer was followed by a scintillator hodoscope (HOD) which provided time measurements for charged particles with a resolution of $\sim$ 150 ps. Further downstream was a liquid krypton electromagnetic

* Presented at "Excited QCD 2019", Schladming, Austria, January 30–February 3, 2019.

† Cambridge, CERN, Dubna, Chicago, Edinburgh, Ferrara, Firenze, Mainz, Northwestern, Perugia, Pisa, Saclay, Siegen, Torino, Wien.

calorimeter (LKr). The energy resolution of LKr for photons and electrons was $\sigma_E/E = (3.2/\sqrt{E} \oplus 9.0/E \oplus 0.42)\%$ (E is in GeV). A muon veto (MUV), made of 3 scintillator planes and iron, aimed at tagging muons.

2. Measurement of the K_{l3} form factors

Semileptonic kaon decays $K^{\pm} \to \pi^0 l^{\pm} \nu$ (K_{l3}, $l = \mu, e$) offer the most precise determination of the CKM matrix element $|V_{US}|$ [3] that require both a branching ratio and a form factors (FFs) experimental measurement. New NA48/2 K_{l3} precision FFs measurement result is presented in [4].

In the approximation of negligible electromagnetic effects, the K_{l3} differential rate as a function of the lepton and pion energies in the kaon rest frame can be parameterised [5] in terms of the vector $f_+(t)$ and scalar $f_0(t)$ FFs, where $t = (P_K - P_\pi)^2$

$$\frac{\mathrm{d}^2\,\Gamma\left(K^{\pm}_{l3}\right)}{\mathrm{d}E_l\,\mathrm{d}E_\pi} = \rho(E_l, E_\pi) \propto \left(A\,|f_+(t)|^2 + B\,f_+(t)f_-(t) + C\,|f_-(t)|^2\right)\,, \quad (1)$$

here, E_l and E_π are the lepton and pion energies in the kaon rest frame; $f_-(t) = (f_0(t) - f_+(t))(m_K^2 - m_{\pi^0}^2)/t$; m_K and m_{π^0} are the $K^{\pm}$ and π^0 masses [6]. The kinematic factors are $A = m_K(2E_lE_\nu - m_K(E_\pi^{\max} - E_\pi)) + m_l^2((E_\pi^{\max} - E_\pi)/4 - E_\nu)$, $B = m_l^2(E_\nu - (E_\pi^{\max} - E_\pi)/2)$, $C = m_l^2(E_\pi^{\max} - E_\pi)/4$. Here, $E_\pi^{\max} = (m_K^2 + m_\pi^2 - m_l^2)/(2m_K)$ (m_l is the lepton mass), and $E_\nu = m_K - E_l - E_\pi$ is a neutrino energy in the kaon rest frame. For K_{e3}, the terms B and C are negligible due to small $e^{\pm}$ mass, so in this case, only the vector FF contributes to $\rho(E_l, E_\pi)$.

Three K_{l3} FF parameterizations were used: (1) Taylor expansion [6] ($f_+(t) = 1 + \lambda'_+ t/m_\pi^2 + \frac{1}{2}\lambda''_+(t/m_\pi^2)^2$, $f_0(t) = 1 + \lambda'_0 t/m_\pi^2$), (2) pole [7] ($f_+(t) = \frac{m_{\mathrm{V}}^2}{(m_{\mathrm{V}}^2 - t)}$, $f_0(t) = \frac{m_{\mathrm{S}}^2}{(m_{\mathrm{S}}^2 - t)}$), (3) dispersive [8] ($f_+(t) = \exp(\frac{(\Lambda_+ + H(t))t}{m_\pi^2}$, $f_0(t) = \exp(\frac{(\ln[C] - G(t))t}{(m_K^2 - m_\pi^2)})$, where m_π is the mass of charged pion. The external functions $H(t)$, $G(t)$ of the dispersive parameterization are taken from [8].

For the K_{l3} event selection, LKr energy clusters and charged particle tracks are reconstructed as described in [1]. An event is considered as a K_{l3} candidate, if there are at least 2 LKr clusters consistent with γ, the energy being above 3 GeV, and the sum of their energies above 15 GeV, ensuring high trigger efficiency. The distances between a photon cluster and the track impact point at the LKr front plane of each in-time (within ± 10 ns) track should be larger than 15 cm. The γ candidates are required to be at least 8 cm away from the LKr edges. The Z_n position of the $\pi^0 \to \gamma\gamma$ decay vertex is computed from photon candidate positions and energies assuming the nominal π^0 mass [6].

At least one charged track is required with a minimum momentum of 5 GeV/c (10 GeV/c) for the $K_{e3}(K_{\mu 3})$ selection. Tracks with $E_{\rm LKr}/P_{\rm DCH} > 0.9$ are identified as $e^{\pm}$, otherwise the $\mu^{\pm}$ identification hypothesis is checked using MUV information. The transverse position of the decay vertex is defined by the track coordinates at Z_n. A loose Z_n-dependent cut is applied to the distance between the vertex and the beam axis. The kaon momentum P_K is computed under the assumptions of the kaon line of flight along the beam axis and a massless missing neutrino. From the two possible P_K solutions, the one closer to the beam momentum central value is chosen.

The background contribution has been estimated using the Geant3-based [9] Monte Carlo (MC) simulation. For K_{e3}, the background from $K^{\pm} \to \pi^{\pm}\pi^0$ (2π) significantly contributes to the signal. For $K_{\mu 3}$ selection, essential background may come from 2π decays with a subsequent $\pi^{\pm} \to \mu^{\pm}\bar{\nu}$ decay. For both $K_{\mu 3}$ and K_{e3} samples, the $K^{\pm} \to \pi^{\pm}\pi^0\pi^0$ decays can contribute to the background. Samples of 4.4×10^6 K_{e3} $(2.3 \times 10^6$ $K_{\mu 3})$ events with less than 1 per mille (∼2 per mille) background have been selected.

Monte Carlo K_{l3} samples have been simulated using the KLOE generator [10] modified for K_{e3} according to the model-independent (universal) radiative correction proposed in [11]. The concept of universal radiative correction assumes the extraction of effective FFs that absorb all the high-order interplay between the QED and QCD effects. For the $K_{\mu 3}$ mode, no considerable disagreement was found between the generator [10] output and universal correction [11]. The $K_{\mu 3}$ generator is found to conform universal correction from [11] within the precision defined by statistics, so for this mode, no universal radiative corrections were applied.

TABLE I

FF results of the joint $K^{\pm}_{l3}$ analysis. The correlations include both statistical and systematic uncertainties. The units of λ'_+, λ''_+, λ_0, Λ_+ and $\ln C$ values and errors are 10^{-3}. The units of $m_{\rm V}$ and $m_{\rm S}$ values and errors are MeV/c^2.

	λ'_+	λ''_+	λ_0	$m_{\rm V}$	$m_{\rm S}$	Λ_+	$\ln C$
Central values	24.24	1.67	14.47	884.4	1208.3	24.99	183.65
Stat. error	0.75	0.29	0.63	3.1	21.2	0.20	5.92
Syst. error	1.30	0.41	1.17	6.7	47.5	0.62	14.25
Total error	1.50	0.50	1.32	7.4	52.1	0.65	15.43
Corr. coefficient	−0.934 (λ'_+/λ''_+) 0.118 (λ'_+/λ_0) 0.091 (λ''_+/λ_0)			0.374		0.354	
χ^2/NDF	979.6/1070			979.3/1071		979.7/1071	

The K_{l3} form factors were fitted by means of simulated events reweighting [4] for each iteration of the fit minimizing the simulated Dalitz plots deviation from the corresponding data plots. The fit is performed separately for the K_{e3} and $K_{\mu 3}$ Dalitz plots or jointly by extending the deviation estimator Ξ^2 summation over both Dalitz plots and using a common set of fit parameters. The joint K_{l3} form factor results are shown in Table I.

3. First observation of the $K^{\pm} \to \pi^{\pm}\pi^0 e^+ e^-$ decay

The radiative decay $K^{\pm} \to \pi^{\pm}\pi^0 e^+ e^-$ proceeds via a mechanism $K^{\pm} \to \pi^+\pi^0\gamma^*(\gamma^* \to e^+e^-)$ and has not been observed so far. The first observation is presented here and published in [12]. Signal events are selected concurrently with normalization events $K^{\pm} \to \pi^{\pm}\pi^0$ followed by π^0 Dalitz decay $\pi^0 \to \gamma e^+ e^-$ ($\pi^0_{\rm D}$).

Both signal and normalization candidates are reconstructed from three-track vertices with the track reconstructed momenta in the range of 2–60 GeV/c. The tracks are required to be in time within 5 ns of each other using the HOD time associated to each of the considered tracks. Any track-to-track distance at DCH1 should be larger than 2 cm to suppress photon conversions to an e^+e^- pair in the upstream material. Events with all three tracks hitting the same HOD quadrant are rejected by the trigger algorithms.

Energy clusters in LKr without associated track, in time within 5 ns with the vertex time are identified as the photon candidates. The photon energy should be above 2 GeV.

The $\gamma\gamma$ invariant mass M_{π^0} of signal events ($\gamma e^+ e^-$ for normalization events) is required to be within ± 15 MeV/c^2 from the π^0 PDG mass [6], and the $M_{\pi^{\pm}\pi^0 e^+ e^-}$ invariant mass denoted as M_K to be within ± 45 MeV/c^2 from the $K^{\pm}$ PDG mass. The total momentum is required to be in the range of 54–66 GeV/c.

The correlation between the M_{π^0} and M_K defines a kinematic constraint $|M_{\pi^0} - 0.42 M_K + 73.2| < 6$ MeV/c^2 (see Fig. 1) allowing particle identification without using $E_{\rm LKr}/P_{\rm DCH}$ requirements, therefore increasing the acceptance of low momentum tracks.

Main background sources are $K^{\pm} \to \pi^{\pm}\pi^0\pi^0_{\rm D}$ (with a lost γ) and $K^{\pm} \to \pi^{\pm}\pi^0_{\rm D}$ (with an extra accidental γ combined with the Dalitz decay γ leading to imitation of a $\pi^0 \to \gamma\gamma$ decay). The first background is additionally suppressed by requiring the squared invariant mass of the $\pi^{\pm}\pi^0$ system to be larger than 0.12 GeV$^2/c^4$. To reject further the second background source, both possible invariant masses $M_{ee\gamma}$ are required to be more than 7 MeV/c^2 away from the π^0 PDG mass. The 0.15% background to normalization is due to $K^{\pm} \to \mu^{\pm}\nu\pi^0_{\rm D}$ and $K^{\pm} \to e^{\pm}\nu\pi^0_{\rm D}$ misreconstructed events, where the pion mass is assigned to the lepton candidate.

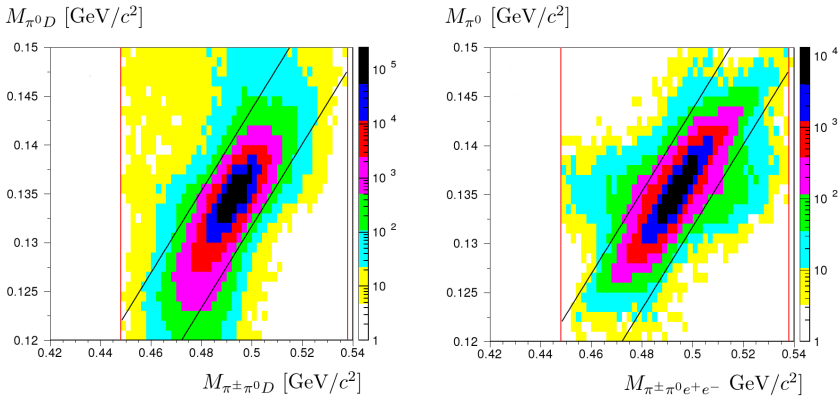

Fig. 1. Left plot: normalization simulated candidates in the plane of reconstructed masses ($M_{\pi^\pm\pi^0 D}$, $M_{\pi^0 D}$). Right plot: signal simulated candidates in the plane of reconstructed masses ($M_{\pi^\pm\pi^0 e^+e^-}$, M_{π^0}). The vertical lines and the slanted bands correspond to the selection constraints.

Samples of 4919 signal candidates and 16.3×10^6 normalization $K_{2\pi D}$ candidates have been selected from an exposure to 1.7×10^{11} kaon decays collected in 2003–2004. The background contamination estimated from simulation is 4.9% in the signal mode and 0.11% in the normalization mode. Reconstructed e^+e^- invariant mass distributions for the normalization and signal candidates are shown in Fig. 2. Expected background, normalization and signal histograms, normalized to the number of observed candidates, show a good agreement with the data distributions.

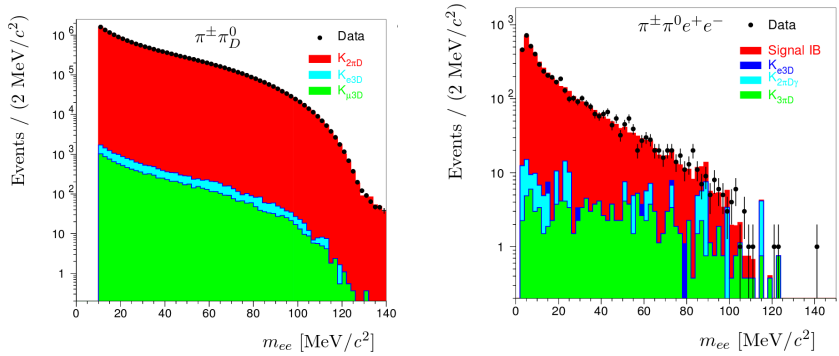

Fig. 2. Reconstructed e^+e^- invariant mass distributions for the normalization $\pi^\pm\pi^0 D$ candidates (left) and for the signal $\pi^\pm\pi^0 e^+e^-$ events (right).

The final result for the branching ratio is $\mathrm{BR}(K^\pm \to \pi^+\pi^0 e^+e^-) = (4.23 \pm 0.06_{\mathrm{stat}} \pm 0.03_{\mathrm{syst}} \pm 0.13_{\mathrm{ext}}) \times 10^{-6}$, where the systematic error includes uncertainties related to acceptances, trigger efficiencies and radiative

corrections. The external error is due to the normalization mode branching ratio uncertainty [6]. The obtained result is in agreement with the theoretical prediction [13].

Study of the kinematic space of the decay has been performed to extract information on the fraction of magnetic M and interference inner bremsstrahlung and electric IB–E contributions with respect to inner bremsstrahlung IB. The relative contribution, $(\mathrm{M})/\mathrm{IB} = (1.14 \pm 0.43_{\mathrm{stat}}) \times 10^2$, is found consistent with the theoretical expectation. The $(\mathrm{IB–E})/\mathrm{IB} = (0.14 \pm 0.36_{\mathrm{stat}}) \times 10^2$ is also in agreement with the theoretical prediction [14]. Several CP-violating asymmetries and a long-distance P-violating asymmetry [13] have been evaluated and found to be consistent with zero.

4. Conclusion

K_{l3} FFs measurement is performed by NA48/2 on the 4.4×10^6 ($K^{\pm}_{e3}$) and 2.3×10^6 ($K^{\pm}_{\mu 3}$) selected events. The obtained precision is competitive with the previous measurements for the $K_{\mu 3}$ mode, and is improved for K_{e3}, resulting in the most precise combined K_{l3} result [4].

The decay $K\pm \to \pi^{\pm}\pi^0 e^+ e^-$ was observed for the first time. Based on 4919 candidates with 4.9% background contamination, the branching ratio is measured to be $(4.24 \pm 0.15) \times 10^{-6}$, in good agreement with ChPT-based theoretical predictions. The ratios (M)/IB and (IB–E)/IB were measured and found to be consistent with theoretical predictions. The CP-violating asymmetries and a long-distance P-violating asymmetry [13] have been found to be consistent with zero.

REFERENCES

[1] J.R. Batley *et al.*, *Eur. Phys. J. C* **52**, 875 (2007).
[2] V. Fanti *et al.*, *Nucl. Instrum. Methods Phys. Res. A* **574**, 433 (2007).
[3] M. Antonelli *et al.*, *Eur. Phys. J. C* **69**, 399 (2010).
[4] J.R. Batley *et al.*, *J. High Energy Phys.* **1810**, 150 (2018).
[5] L.-M. Chounet, J.-M. Gaillard, M. Gaillard, *Phys. Rep.* **4**, 199 (1972).
[6] C. Patrignani *et al.* [Particle Data Group], *Chin. Phys. C* **40**, 100001 (2016).
[7] P. Lichard, *Phys. Rev. D* **55**, 5385 (1997).
[8] V. Bernard, M. Oertel, E. Passemar, J. Stern, *Phys. Rev. D* **80**, 034034 (2009).
[9] Geant detector description and simulation tool, CERN program library long writeup W5013, CERN, Geneva, Switzerland, 1994.
[10] C. Gatti, *Eur. Phys. J. C* **45**, 417 (2006).
[11] V. Cirigliano *et al.*, *Eur. Phys. J. C* **23**, 121 (2002).
[12] J.R. Batley *et al.*, *Phys. Lett. B* **788**, 552 (2019).
[13] L. Cappiello, O. Catà, G. D'Ambrosio, D.N. Gao, *Eur. Phys. J. C* **72**, 1872 (2012).
[14] L. Cappiello, O. Catà, G. D'Ambrosio, *Eur. Phys. J. C* **78**, 265 (2018).